Biogeosciences Discuss., 8, 9639–9669, 2011
www.biogeosciences-discuss.net/8/9639/2011/
doi:10.5194/bgd-8-9639-2011

Biogeosciences Discussions

Gas properties of winter lake ice in Northern Sweden: biogeochemical processes and implication for carbon gas release

T. Boereboom[1], **M. Depoorter**[2], **S. Coppens**[1], **and J.-L. Tison**[1]

[1]Laboratoire de Glaciologie, Université Libre de Bruxelles, Belgium
[2]Bristol Glaciology Centre, University of Bristol, UK

Received: 14 September 2011 – Accepted: 17 September 2011
– Published: 27 September 2011

Correspondence to: T. Boereboom (thierry.boereboom@ulb.ac.be)

Published by Copernicus Publications on behalf of the European Geosciences Union.

Abstract

This paper describes gas composition, total gas content and bubbles characteristics in winter lake ice for four adjacent lakes in a discontinuous permafrost area. Our gas mixing ratios suggest that gas exchange occurs between the bubbles and the water before entrapment in the ice. Comparison between lakes enabled us to identify 2 major "bubbling events" shown to be related to a regional drop of atmospheric pressure. Further comparison demonstrates that winter lake gas content is strongly dependent on hydrological connections: according to their closed/open status with regards to water exchange, lakes build up more or less greenhouse gases (GHG) in their water and ice cover during the winter, and release it during spring melt. These discrepancies between lakes need to be taken into account when establishing a budget for permafrost regions. Our analysis allows us to present a new classification of bubbles, according to their gas properties. Our methane emission budget (from $6.52\,10^{-5}$ to $12.7\,\mathrm{mg\,CH_4\,m^{-2}\,d^{-1}}$) for the three months of winter ice cover is complementary to the other budget estimates, taking into account the variability of the gas distribution in the ice and between the various types of lakes.

Most available studies on boreal lakes have focused on quantifying GHG emissions from sediment by means of various systems collecting gases at the lake surface, and this mainly during the summer "open water" period. Only few of these have looked at the gas enclosed in the winter ice-cover itself. Our approach enables us to integrate, for the first time, the history of winter gas emission for this type of lakes.

1 Introduction

Lakes in subarctic environments are affected by and contribute to the current global warming. In permafrost areas, lakes are net emitters of methane and carbon dioxide, which both contribute to the greenhouse effect. Lakes areas in these regions represent up to 30 % of land surface (e.g. Walter et al., 2008) and this ratio could increase in the coming years, as permafrost degradation supports lakes development. These lakes, embedded in recently unfrozen sediments, sustain anaerobic condition favouring methane emissions. The latter have been largely studied in recent years (e.g. review Table in Walter et al., 2010), since they are recognized as an important contributor to the greenhouse effect. Nevertheless, CH_4 emissions are still not included in Global Climate Models (GCMs) because of large uncertainties (IPCC, 2007).

Methane is produced in the sediment, where it results from acetate fermentation or CO_2 reduction in anaerobic environments. It reaches the atmosphere through the plants system, by bubbling or by diffusion through the water column. Bubbling is easily identifiable on the water surface mainly in spring and summer and is largely studied using various techniques (floating chambers, bubble traps, inverted funnel systems...). During winter periods, bubbles are enclosed in the ice, indicating that methane emission from sediment is still an active process. In peculiar situations, the emissions are so intense that they inhibit the ice formation (hotspot). The transit in the water column can induce several biochemical reactions. Methane can be oxidized to CO_2 in an oxic medium, via methanotrophic bacteria, and lakes can supply such an environment depending on their geometry and hydrology. Due to the temperature of the maximum of density of fresh water (+4 °C), lakes in periglacial areas are known as dimictic i.e. presenting two periods of stratification and two overturn events, one during spring, soon after ice cover melting, and the other when the winter begins (Bastviken et al., 2004; Casper et al., 2000). Stratification favours the development of an anoxic layer whereas overturning causes oxygenation in the water column. Lakes are therefore mainly stratified during the winter and the ice cover will further limit atmosphere – water interactions. This closed system will result in the buildup of CO_2 and CH_4 concentrations in the water and mixing ratios in the ice. During spring, these gases will be released to the atmosphere. Methane will resituate mainly from ice melting and bubbles emissions while carbon dioxide will release rather from gas re-equilibration as water overturns (Casper et al., 2000; Michmerhuizen et al., 1996; Phelps et al., 1998). Indeed, the solubility of these two gases is very different: in fresh water at 20 °C pure CH_4 saturation is

BGD
8, 9639–9669, 2011

about 1.6 mol m^{-3} whilst the CO_2 saturation is reached at about 39 mol m^{-3}. Moreover, lakes characteristics (size, depth, water circulation, hydrological system ...) should also influence gas emissions, a process which has only been scarcely described.

Most studies have performed measurements on open water and only a few focused on the gas properties of the lake ice cover. Here we present, to our knowledge, the first high resolution profiles of the total gas content and gas composition of lake ice from 4 lakes in Northern Sweden. This approach enables us to discuss gas enclosure in lake ice during the whole 3 months period of ice growth. Interactions between the water column and the ice cover are also shown to control bubbles composition as well as the intra- and inter-lake variability in hydrodynamic regimes.

2 Study area and sampling

The four investigated lakes are embedded in the Stordalen Mire peat bog area (68°21′ N, 19°02′ E), near the Torneträsk lake (Fig. 1). It is a sporadic or discontinuous permafrost area (Akerman and Johansson, 2008; Johansson et al., 2006a, b) with low vegetation (Sonesson et al., 1980; Svensson et al., 1999). Transects from the center to the bank have been performed for each lake, in order to study the intra-lake variability. Ice cores were extracted along these transects. Several of these were analyzed for their gas properties. In this paper, we present 3 cores from Lake 2 and 4 cores from the other lakes. Figure 2 shows the ice cores locations, ice thickness and the depth profiles at times of core retrieval. We also collected about fifteen individual "ice embedded large flat bubbles". These ranging from 2 to 5 cm in diameter were outcropping near the surface, but not especially along the transect studied. While Lake 1 and Lake 4 appear disconnected from any obvious water circulation pattern, Lake 2 and Lake 3 are not. We will refer to this contrast by using the "closed" vs. "open" lake terminology, respectively. Lake 1, Lake 2 and Lake 3 display a small surface area of 0.01 to 0.02 km^2. Lake 4 is quite larger (0.19 km^2). According to water connections in the winter, Lake 1 is closed. Lake 2 has a semi-open character because of its connection to another lake downstream (see Fig. 1). Its profile hasn't been documented here in details, but its maximum depth is known to be 5 meters (Kokfelt et al., 2009). Lake 3 is relatively deep (5 m) for its size. It is an open system as it benefits from water fluxes throughout the winter. Incoming water originates from the river (see Fig. 1), and flows into the NW lake (pers. com. David Olefelt). Lake 4 consists of three interconnected areas and seems to behave as a closed system. Only the southern area has been studied in this paper. There, the lake is shallow with a maximum surveyed depth of 105 cm.

The lake ice was drilled at the end of the winter in the last days of March 2008, near to maximum ice extent and thickness.

3 Methods

The drilling was performed using a SIPRE-type ice auger (7.5 cm in diameter), the samples were cut with a band saw in a –20 °C cold room. Horizontal thick sections (±8 cm × 7 cm × 0.5 cm) were processed continuously along the ice cores using a Leitz 1400 microtome following the standard procedures from Langway (1958).

Gases entrapped in the ice were analysed every 5 cm (30 g–50 g) for their total volume and composition (CO_2, O_2, N_2 and CH_4). Gas composition was measured by gas chromatography (Interscience Trace GC) using a FID detector for CO_2 and CH_4 and a TCD detector for O_2 and N_2. The gases were collected using the dry-extraction technique described in Raynaud et al. (1982) and Barnola et al. (1983). Precision of the measurements is 2.5 % for CO_2, 0.4 % for O_2 and N_2, and 3 % for CH_4. Total gas content was determined using a Toepler pump, applying the melting-refreezing extraction technique described in Martinerie et al. (1994). The associated total gas volume error is ≤5 %.

Ice thickness and depth measurements were performed with an ice thickness gauge designed by © Kovacs enterprises (precision: ± 1 cm).

BGD
8, 9639–9669, 2011

4 Results

4.1 Ice characteristics

Figure 3 summarizes the ice and bubbles morphology from the 15 studied ice cores, as seen in transmitted light through the 0.5 cm thick sections. Visually, bubble shapes show a large variability. However, 6 major ice types have been identified, on the basis of their bubble characteristics. Type 1 is peculiar and scarce, we call it "snow ice", because this ice type clearly results from liquid water infiltration and refreezing in the snow cover at the lake surface. We observed this ice type at the very top few millimeters of most cores, but especially core 1 on Lake 3. Type 2 corresponds to ice without visible bubbles. We will refer to it as "clear ice", and it has been found in most part of the Lake 3 ice cover but also in small sections of Lake 1 and Lake 2 cores. Ice with elongated cylindrical bubbles (ice type 3) is predominant in Lake 4 (e.g. around 40 cm depth) but also in some sections of Lake 1 and Lake 2. Ice with spherical or nut shape bubbles is found at the bottom of all the shallow depths cores of Lake 1. Note that this ice type 4 is quite rich in bubbles.

Some core sections clearly display a mixture of cylindrical, spherical, and nut shaped bubbles as for example, section 47–65 cm depth in core 6 of Lake 1. This fifth ice type is called "mixed ice". Finally, as described earlier in the paper, we can sometimes observe a sixth ice type containing bigger isolated large flat bubbles (see, top of core 2 in Lake 1). These bubbles can be very large with a diameter of up to a meter and are generally filled up by small hexagonal ice crystals, giving a whitish appearance to the bubble. These crystals, resulting probably from the inverse sublimation process after bubbles formation, reduce the gas volume in the latter. In this work, the maximum bubble size analyzed was obviously constrained by the corer diameter.

The genesis of the various ice types described above will be discussed further in this paper, but we would like to emphasize at this stage how the spatial distribution of these ice types varies within each lake as well as in between them. In Lake 1, the bubble content drastically increases between 50 cm depth and the bottom of cores 2, 4 and 6

BGD
8, 9639–9669, 2011

where we find ice type 4 and 5. This feature does not exist in core 9, sampled above deeper water (Fig. 2), where the bottom part is made of "clear ice" (ice type 2). Of all lakes studied, Lake 3 shows the lowest bubble density. It predominantly consists of ice type 2 (clear ice) except for two discrete zones with cylindrical elongated bubbles (around 30 cm depth and at the top of core 8) (Fig. 3). The sub horizontal lines in core 1 from the same lake are not bubble but natural fractures. Lake 4, which is nearly frozen to bottom along the whole profile (Fig. 2), on the contrary, shows a large density of bubbles for all cores at all depths, dominated by ice type 3 (elongated bubbles) and mixed ice (ice type 5). Finally, in all of the 15 ice cores for which thick sections have been made, we can identify a common zone of higher bubble density at about 30 cm depth (Fig. 3).

4.2 Gas composition

Gas composition has been measured continuously and at high resolution in a selected core for each lake (cores 4, 1, 1 and 4 for respectively lakes 1, 2, 3 and 4), but also in individual samples of the large flat bubbles (ice type 6). Results are presented in Fig. 4.

Methane mixing ratios (Fig. 4a) vary largely between 3 ppm and 47 %. Large flat bubbles show the maximum mixing ratios whereas profiles values are at the level of tens to hundreds of ppm with a few peaks around 10 or 20 %. We observe an increase for all lakes (except for Lake 3) around 25 cm depth. Methane mixing ratios for lakes 1 and 4 increase with depth whereas the mixing ratios of lakes 2 and 3 remain low.

Unlike methane, the range of CO_2 mixing ratios (Fig. 4b) is the same for the large flat bubbles (ice type 6) as for the profiles in the cores. To the single exception of the top of the lake 3 core 1 (9 %), it varies between 200 and 4000 ppm. For all lakes, however, the CO_2 mixing ratio increases with depth with a maximum value of 46 600 ppm.

Oxygen mixing ratio (Fig. 4c left) is about 20 % near the surface of all lakes, to the exception of some large flat bubbles with lower values at 10 %. In Lake 1, 2 and 4, there is also a relative minimum at 10–15 % around 25 cm depth and a clear decrease again between 40 cm depth and the bottom of the cores to mixing ratios of 5 to 15 %. Lake 3, on the contrary, is remarkably stable at a value of 21 %, close to the atmospheric value, although with very low total gas content (see Fig. 4e and Sect. 4.3).

Nitrogen mixing ratios (Fig. 4c right) are around 78 % near the lakes surface and, in most cases, logically evolve in opposition to the O_2 mixing ratio (since they are usually the dominant species).

The O_2/N_2 ratio (Fig. 4d) varies between 0.084 and 0.33 for ice type 6 and between 0.26 and 0.34 for the cores profiles near the lakes surface. The ratio decreases with depth to a minimum value of 0.05 for Lake 1, 2 and 4 whereas it remains constant for Lake 3 with a value of 0.28. The decrease of the ratio actually always reflects a decrease in the oxygen, which is confirmed by a comparison of O_2 and N_2 concentrations in the water (not shown). For Lake 1, 2 and 4 repeated changes of the ratio are seen throughout the depth, superimposed to the general trend.

4.3 Total gas content

The total gas content results of Fig. 4e should be taken with care and generally considered as a minimum values. The extraction process indeed underestimates the total gas content from the samples, by cutting through bubbles on sampling and therefore losing their gas content. This error becomes significant for ice with cylindrical elongated bubbles. On the other hand, we do not show values for ice type 6 since it clearly has no meaning.

This being said, our values are in the same range or slightly higher than other studies previously performed on lake ice (e.g. Lorrain et al., 1999, 2002).

5 Discussion

5.1 A new lake ice type classification based on bubbles properties

Bubble shapes in lake ice have already been discussed at length by several authors (Adams et al., 1998; Bari and Hallett, 1974; Carte, 1961; Gow and Langston, 1977). These authors suggest that bubble shapes and density will result from a balance between the rate of advance of the freezing front, and the solubility state of the gases in the liquid reservoir ahead. Basically, with a faster freezing front, bubbles will form and be rather elongated and perpendicular to the ice front. They can sometimes be accompanied by "nut shape" bubbles. At low freezing rates, the ice can be devoid of bubbles if, the expulsed gases are able to diffuse and dissolve in the water reservoir. Furthermore, in permafrost areas, large bubbles resulting from sediment degassing will also be a common feature (Walter et al., 2006).

The data collected in this paper enable us to propose a new "process-driven" lake ice type classification based on bubbles characteristics and associated gas composition. This classification, summarized in Fig. 5, combines the influence of dissolved gases in the water, sediment degassing and gas-water interactions within the water column. It differs from the one established by Walter et al. (2006), in that the bubble size ranges are different. Indeed, in this work, we are limited by the sampling method to bubbles that are smaller than 5 cm in diameter. Each of the 6 ice types described in Sect. 4 and Fig. 5 can then be associated to a specific genetic process for the bubble inclusions. Type 1 (snow ice) is formed by liquid water infiltration in snow blown at the surface of the lake and subsequent refreezing. Type 2 (clear ice) is typical of lake ice formed in conditions of slower freezing (favouring diffusion ahead of the freezing front) of a water reservoir which is undersaturated or not supersaturated enough for bubble nucleation to take place. Type 3 (elongated bubbles) and 4 (spherical and nuts shape bubbles) is typical lake ice where bubbles solely result from the capture of exsoluted gases as the boundary layer ahead of the ice-water interface gets strongly supersaturated from impurity rejection by the ice (higher freezing rates, closed system freezing). Type 6 ice

BGD
8, 9639–9669, 2011

(large flat bubbles) is the signature of an ebullition process from the sediment on the lake floor, captured at the base of the ice cover. Finally, type 5 is the expected mixed facies when both exsolution and ebullition contribute to the bubble content at the same location.

5.2 Depth dependency of the gas composition

In parallel with the different bubble characteristics of the various ice types, the composition of these gaseous inclusions varies with depth in most cases. Figure 4c, for example, shows a clear decrease of the oxygen mixing ratio from 20 % near the surface to about 5 to 10 % at 70 cm depth. Simultaneously, the CO_2 mixing ratio increases from 500–1500 ppm up to a maximum value of 40 000 ppm. Oxygen decrease is a known phenomenon in stratified lakes (e.g. Casper et al., 2000) and generally attributed to respiration process in the liquid phase.

In order to decipher the impact of biogenic processes from the mere evolution of gas properties under the specific hydrodynamic conditions of a freezing lake, we have estimated the evolution of gas concentration in water and of gas mixing ratios in water and ice, in the absence of biological activity, using the following approach. Hypothesizing that the initial gas composition of the lake water is in equilibrium with the atmosphere and that the reservoir evolves as a closed system, one can compute, using Henry's law (1) and the total gas content measured in the ice (Fig. 4e), the theoretical evolution of gas concentrations ($\text{mol}\,\text{l}^{-1}$) in the reservoir with depth applying a simple mass balance between ice and water. This is shown as grey diamonds for oxygen, carbon dioxide and methane in Fig. 6 (nitrogen not shown).

$$c = k_h \cdot p \qquad (1)$$

where c = dissolved gas concentration ($\text{mol}\,\text{l}^{-1}$)

k_h = Henry's constant ($\text{mol}\,\text{l}^{-1}\,\text{atm}^{-1}$)

p = gas partial pressure (atm)

BGD
8, 9639–9669, 2011

k_h values and temperature corrections were applied as recommended in Sander's review (1999). Further, theoretical mixing ratios in water and ice (using Henry's law again) can be reconstructed, as shown for all gases in Fig. 7. Note that these computations neglect potential selective diffusion ahead of the freezing front, which might affect the results by a factor of 2 to 3 at high freezing rates (top layers), considering respective diffusion coefficient of various species. Care should also be taken in discussing these curves in the specific case of carbon dioxide, since our calculations did not take into account the re-equilibration of the carbonate system in the water, as freezing concentrates carbon dioxide in the remaining reservoir. Indeed, at normal pH, the major part of carbon dissolved in the water is under the HCO_3^- form. Our theoretical CO_2 curves in Figs. 6 and 7 based on a simple conservative mass balance between ice and water in a closed system therefore potentially overestimate the increases of CO_2 concentrations in water and the mixing ratios in water and ice as the reservoir closes.

As expected from the limited amount of gas enclosed as bubbles in the ice, theoretical concentrations in water regularly increase with depth (Fig. 6, N_2 not shown). Also, following relative solubilities, mixing ratio increase for all gases apart from nitrogen, since the latter is the dominant species and the least soluble (Fig. 7a). Maximum water concentrations are reached at the bottom of Lake 1 with value of 5.2 ppm in CH_4, 55 000 ppm in CO_2 and 55 % for O_2, resulting in ice bubbles mixing ratios of respectively 3.2 ppm, 1100 ppm and 36.9 %. Another salient feature of Fig. 7 is the behavior of Lake 3 showing only little changes with depth, as expected from its deeper waters (Fig. 2). Now, real gas concentrations in the water can also be reconstructed using the observed gas mixing ratios in the ice and applying Henry's law. This is shown for O_2, CO_2 and CH_4 as grey triangles downwards in Fig. 6.

Are the observed ice gas mixing ratio profiles of Fig. 4 coherent with the closed system theoretical evolution shown in Fig. 7b? Methane shows a wide range of values (from a few ppm to 100 000) and no systematic increasing trend with depth. Only exceptionally is the maximum "closed system" value of few ppm observed (here as a minimum in the profiles), and not necessary at the bottom of the ice cover. This clearly

BGD
8, 9639–9669, 2011

suggests that exsolution is not the dominant process in controlling methane mixing ratios in the ice, but rather the varying contribution of ebullition process.

Comparing observed to theoretical profiles for carbon dioxide in lakes 1, 2 and 4 shows a similar trend of increasing mixing ratio in ice (Fig. 7b) and concentrations in water (Fig. 6, middle panel). However, again, in both cases, observed values can be higher than theoretical ones by up to an order of magnitude, with considerable superimposed variability. An additional source of carbon dioxide is therefore required, and this from the very beginning of the growth season as shown by the lake water supersaturation level of the reconstructed water concentrations from bubbles in the ice (Fig. 6, central panel, grey diamonds). Could this be the result of respiration processes in the reservoir? The behavior of dissolved oxygen is worth considering in that respect. Indeed, instead of showing the expected increase of mixing ratio (Fig. 7a) and concentration in water (Fig. 6, left panel, grey diamonds) with depth, reconstructed water concentrations actually slightly decrease in lakes 1, 2 and 4. This could be interpreted as the signature of respiration. Looking at relative increase of CO_2 and decrease of O_2 in Fig. 6 reveals important contrasts between lakes and between depths in a given lake. In the lower half of lakes 2 and 4 oxygen loss and CO_2 gain are in relative balance, which does not preclude a respiration control in the water column during ice growth, especially that we know that some of the CO_2 produced could have moved to the HCO_3^- pool. On the contrary, in the upper half of the ice cover from the same lakes, negligible amounts of oxygen are lost, whilst excess carbon dioxide is present. For Lake 1, CO_2 gain is at all times in excess of the O_2 loss, also suggesting an alternative source to respiration for CO_2, from the very beginning of the lake ice growth. Finally, Lake 3, which has been described as a relatively open system, shows three distinct sections; a lower one coherent with respiration processes (as in lakes 2 and 4), a top section where the CO_2 gain overwhelms the (negligible) O_2 loss (as in all other lakes), and a middle section where CO_2 concentrations are closed to the theoretical closed system evolution.

BGD
8, 9639–9669, 2011

To summarize, dissolved CO_2 concentrations in the waters of lakes 2, 3 and 4 can be explained by "in situ" respiration processes for waters generating the lower part of the lake ice cover (late growth), whilst an extra source (as compared to simple equilibrium with atmosphere) is needed for the waters generating the upper part of the lake ice cover (early growth). For Lake 1, this extra source is needed at all times. Although reservoir closure is unable to explain the observed levels of concentration, it could be partly responsible for the general trend of CO_2 concentrations in lakes 1, 2 and 4.

Several mechanisms, other than respiration, can explain the high levels of observed dissolved CO_2 in our lake waters. Gas ebullition from the sediment can certainly contribute to the CO_2 increase. Sulfato-reduction, which is often associated to the methanogenesis process (Fenchel et al., 1998), is also a provider of carbon dioxide and the particular smell of H_2S, another by product of the reaction, has been detected during the field trip. Denitrification, methane oxidation or acetate fermentation can also contribute to the CO_2 content (Stumm and Morgan, 1996). In our case, the similarity of the reconstructed CH_4 and CO_2 concentration profiles in water in most lakes (Fig. 6, middle and right panels) suggest that acetate fermentation might be the dominant extra CO_2 source at work, as opposed to methane oxidation. This also puts forward acetate fermentation as the source for methane. $\delta^{13}C$ and δD isotopic analysis of the CH_4 would of course help in deciphering the sources, but these unfortunately and not available at this time. The generalized CO_2 excess in the surface layer of all lakes could reflect the dynamical instability of the lake waters in the autumn, bringing bottom enriched waters to the lake surface just before the onset of freezing.

The O_2/N_2 ratio (Fig. 4d) actually reflects the changes in the oxygen mixing ratio and can therefore also be used as an indicator of the stratification process in the lake during the winter. But, it can also be a measure of the hydrological regime in the lake (open vs. closed system). For example, Lake 3 shows a constant O_2/N_2 ratio throughout the depth because the input of atmosphere equilibrated waters from the river upstream (Fig. 1) inhibits the changes in oxygen mixing ratios due to the ice cover freeze on (closure) or biological processes as discussed above. It is interesting to note

BGD
8, 9639–9669, 2011

that local CO_2 mixing ratio increases occur at about 50 and 60 cm depth, despite the water circulation. This suggests that these excursions correspond to local ebullition events, as confirmed in the CH_4 profile.

5.3 Ice type dependency of gas mixing ratios

Figure 5 shows contrasted CH_4 and CO_2 signatures for the various ice types described in Sect. 5.1. Only one measurement is available for the "snow ice" (type 1), and it shows the highest CO_2 value of the whole study at 90 000 ppm. This is hard to explain by physical processes only. Figure 7a shows that CO_2values up to 54 000 ppm can be reached for gas dissolved in water during closed system freezing of lake reservoir (at about 70 % freezing). Bulk freezing of residual water from the final stages of closed system freezing of a lake, expelled at the surface through the moat and bathing the snow cover, could therefore lead to such high CO_2 values. This is however quite unlikely, since our "snow ice" was measured at the surface of Lake 3, which was the least "closed". Bacterial respiration of organic matter blown with the snow at the lake ice surface is another plausible explanation. Strangely enough, oxygen does not show the expected concentration decrease if aerobic respiration had been active. Ice types 2 to 4 should span the range of theoretical CO_2 mixing ratios shown in Fig. 7b (400 to 1100 ppm) if the water was initially in equilibrium with the atmosphere. We know from the discussion above that this is not true, and the observed range of 3000 to 4000 ppm is in accordance with exsolution from a lake water displaying the observed excess-CO_2 concentration. The "mixed ice" (type 5), with apparent contribution from both exsolution bubbles and small bubbles resulting from sediment ebullition, shows higher CO_2 and CH_4 mixing ratios as compared to ice type 3 and 4. This suggests that the small bubbles coming from the sediment contribute to increase both the carbon dioxide and the methane content as surmised from the discussion in the previous section. The large flat bubbles (type 6), also derived from sediment ebullition are globally richer in methane but poorer in carbon dioxide. This however does not mean that the amount of carbon dioxide in these bubbles is lower as compared to ice type 5, since the data are shown as mixing ratio (i.e. relative concentration). It is nevertheless disturbing, if ice type 5 is a mixture between ice types 3/4 and 6, that the CO_2 mixing ratio is not at an intermediate value (as does CH_4 in Fig. 5). This suggests that a small fraction of methane (not detectable in Fig. 6) might have been oxidized to CO_2 in the lake environment or in the ice itself.

This underlines that the lake ice cover signature is clearly different from that of ebullition. As illustrated by the contrast between ice type 5 and 6, the least soluble methane dominates ebullition, while carbon dioxide mixing ratio is higher in the lake ice storage. This however needs to be weighed by the overwhelming amount of gas liberated through ebullition, as compared to the one stored in the lake ice.

5.4 Controls on bubble distribution in lake ice

Intra-lake and inter-lake comparison in our dataset shows that there is a control of geometry on the bubble distribution in the ice, which is of potential interest in the perspective of upscaling regional dataset to global carbon budgets. For example, the proximity of the bottom of the lake increases the amount of bubbles in the ice. Figures 2 and 3 indeed show that the lower part of cores C2, C4 and C6 of Lake 1 in shallow areas is rich in bubbles while it is not true for core C9, located above deeper waters. For Lake 4 which is shallow and nearly frozen to the bottom, all ice cores are bubble rich. This suggests that not only the surface area of the lakes (Bastviken et al., 2004; Juutinen et al., 2009), but also their water depth is important in assessing gas productivity on a larger scale.

The hydrological regime of the lake system can also directly impact the gas content in the lake ice. Our study shows that if a lake is part of an open drainage system, the ice can be nearly devoid of gas. Lake 3, which is fed by a river (Fig. 1), and where the water drains into another lake, is a good example (Fig. 3). The three other lakes, on the contrary, are closed or open to another lake without significant water circulation and all show a significative bubble content. In the first case it would be adequate to investigate if the lack of bubbles in the ice is counterbalanced by a supplementary provision in the connected lakes, and to understand how they will affect the quantity (fluxes) and the quality (CH_4 vs. CO_2) of the gases released to the atmosphere.

Finally, in this study, "bank proximity" doesn't seem to affect the bubble distribution despite the fact that lakes can be more methane productive along lakes margins (e.g. Walter et al., 2007). However, all lakes are relatively small, and the situation might be different for larger lakes.

Local events of atmospheric pressure dropping has also been claimed to trigger bubble nucleation in lake ice (Mattson and Likens, 1990; Semiletov, 1999). In this study, we observed two simultaneous bubbling events for the 4 lakes, the first one around 30 cm depth (well documented in Fig. 3) and the second around 60 cm (clearly seen during cores handling). To investigate a potential relationship of these events to marked atmospheric pressure changes, we first need to reconstruct a time line for the buildup of the lake ice cover. A simple (neglecting geothermal heat flux) thermodynamic model for freezing (Hinkel, 1983) has been run, based on Eq. (2):

$$\rho_i \lambda \frac{\delta Z_i}{\delta t} = \frac{T_0 - T_s}{\frac{Z_i}{K_i} + \frac{Z_s}{K_s}} \tag{2}$$

where ρ_i = density of ice ($\mathrm{kg\,m^{-3}}$)
λ = latent heat of fusion ($\mathrm{J\,kg^{-1}}$)
Z_i = ice thickness (m)
Z_s = snow thickness (m)
K_i = thermal conductivity of ice ($\mathrm{W\,m^{-1}\,°C^{-1}}$)
K_s = thermal conductivity of snow ($\mathrm{W\,m^{-1}\,°C^{-1}}$)
T_0 = temperature at ice/water interface (°C)
T_s = surface temperature (°C)
t = duration of constant $T_\mathrm{s}(s)$

The model reconstructs the ice thickness Z_i as a function of the temperature changes and this from the first day of freezing. It has been run both with and without

BGD
8, 9639–9669, 2011

a snow cover to obtain a reasonable prediction of the evolution of the ice cover. The snow cover deduced from snow fall events, was however quite variable between lakes depending on exposition, wind and sublimation processes. It is possible to correlate the observed major bubbling events at around 30 and 60 cm depth with major occurrences of atmospheric pressure drops on Fig. 8 (hatched areas). This confirms that attention should be drawn to major atmospheric pressure events in assessing methane release efficiency from periglacial lakes.

5.5 Assessing a lower bound for lake ice melting contribution to the atmospheric methane budget

In this section we present a "back of the envelope" calculation for a minimum winter contribution of periglacial lakes to methane fluxes to the atmosphere. We rely on our ice type/bubbles classification to perform a budget for methane accumulation in lake ice during the winter. We first calculate the proportion of each ice type in each core considering it as representative for the whole lake ice cover. We then multiply this proportion by the minimum, mean (median) and maximum CH_4 mixing ratio for this type of ice and by the observed mean total gas content of the given ice type. This provides an ice-type weighed concentration of methane in ml CH_4 per gram of ice for each lake. This value is then integrated over the lake ice mass and divided by the lake area and by the number of days of existence of the ice cover. Results are presented in Table 1. Although these values do not represent the actual flux of methane to the atmosphere during the relatively short melting period, they provide a mean winter daily flux, that can be more easily compared to spring-summer flux estimates available in the literature.

We consider these values as minimal for two reasons: (a) because the total gas volume measurements were probably biased towards gas losses (see Subsect. 4.3), and b) because we cannot include the contribution of bubbles above 5 to 6 cm in diameter, which are most likely the larger contributors to the methane budget (Walter et al., 2010). We however consider our results as a measure of the "background contribution" of permafrost lake ice; without the big bubbles events. This work is therefore complementary to other studies focusing on large methane emission observed in spring, due to the ice cover melting and water turnover which releases the excess dissolved gases stored in the water column (Michmerhuizen et al., 1996; Phelps et al., 1998). It is also complementary to studies focusing on larger bubbles in winter lake ice (e.g. Walter et al., 2006, 2007, 2008, 2010).

Our results present a large variability between each lake. Lake 1 shows values ($1.34\,10^{-3}$–$12.7\,mg\,CH_4\,m^{-2}\,d^{-1}$) comparable with some other studies (Bastviken et al., 2004; Kling et al., 1992; Repo et al., 2007; Rudd et al., 1993; Zimov et al., 2001) reporting values from 0.3 to $77\,mg\,CH_4\,m^{-2}\,d^{-1}$. Lakes 2, 3 and 4, on the contrary, show values from $6.52\,10^{-5}$ to $4.4\,mg\,CH_4\,m^{-2}\,d^{-1}$ which are in the lowest range of those reported in most studies on methane fluxes from lakes (values observed from 0 to $3240\,mg\,CH_4\,m^{-2}\,d^{-1}$; Walter et al., 2010). We did expect to find moderate contribution from lake ice in the winter, but we show here that these are not negligible and worth considering in global budget estimations.

6 Conclusions

This work contributes to the study of methane released from lakes in periglacial environments. It provides new results on the winter gas storage associated to the lake ice cover buildup. A new genetic lake ice types classification is proposed, based on bubbles shapes, density and gas composition. It is used to provide a first minimal estimate of methane fluxes associated to winter storage in the lake ice cover, which are complementary to previous studies focusing on spring and summer fluxes from open water sources and studies focusing on large bubbles in lake ice. It is shown that although moderate, as expected, these fluxes are not negligible with respect to other sources.

Gas composition study of the bubbles reveals strong supersaturation of the lake water both in methane and carbon dioxide, especially in the lakes that evolve in near closed system. These high concentrations are thought to mainly result from interaction

BGD
8, 9639–9669, 2011
Gas properties of winter lake ice in Northern Sweden
T. Boereboom et al.

with biological processes in the sediment, of which acetate fermentation would be a likely candidate, given the observed synergy between CO_2 and CH_4 in the profiles. Part of the excess CO_2 could also result from respiration processes, as indicated by oxygen losses, especially during the second half of the ice growth period. Mere closure of the lake reservoir cannot explain the observed concentration excess, but could be partly responsible for the global trend of increasing concentrations with depth in the water and in the ice.

We also demonstrated that lakes geometry and hydrological regime affect the amount and characteristics of gases enclosed in the ice. Finally, we confirm that atmospheric pressure regimes can trigger bubble nucleation and sediment ebullition events and therefore should indeed be considered as a factor in methane release efficiency.

Future work will focus on the stable isotope composition of the bubbles in the different ice types, in order to decipher the relative importance of physico-chemical and biologically mediated processes in controlling the gas properties in permafrost lake ice.

Acknowledgements. We thank the Abisko Scientific Research Station (ANS) in Sweden for their grant and the weather data, the "Fonds de Service pour la Recherche Glaciologique Polaire de l'Université Libre de Bruxelles" and the "Crédits pour Brefs Séjours à l'étranger" of the FNRS for the financial support. We thank Kristina Bäckstrand and David Olefelt for their field knowledge and the personal communications.

References

Adams, E. E., Priscu, J. C., Fritsen, C. H., Smith, S. R. and Brackman, S. T.: Permanent ice covers of the McMurdo Dry Valleys lakes, Antarctica: bubble formation and metamorphism, in Ecosystem Dynamics in a polar desert: the McMurdo Dry Valleys, Antarctica, edited by: Priscu, J., 281–295, American Geophysical Union, Washington, DC., 1998.

Akerman, H. J. and Johansson, M.: Thawing Permafrost and Thicker Active Layers in Subarctic Sweden, Permafrost Periglac., 19, 279–292, 2008.

Bari, S. A. and Hallett, J.: Nucleation and growth of bubbles at an ice-water interface, J. Glaciol., 13, 489–520, 1974.

Barnola, J. M., Raynaud, D., Neftel, A. and Oeschger, H.: Comparison of CO2 measurements by two laboratories on air from bubbles in polar ice, Nature, 303, 410–413, 1983.
Bastviken, D., Cole, J., Pace, M. and Tranvik, L.: Methane emissions from lakes: Dependence of lake characteristics, two regional assessments, and a global estimate, Global Biogeochem. Cy., 18, 12, GB4009, doi:10.1029/2004GB002238, 2004.
Carte, A. E.: Air bubbles in ice, Proceedings of the Physical Society, 77, 757–768, doi:10.1088/0370-1328/77/3/327, 1961.
Casper, P., Maberly, S. C., Hall, G. H., and Finlay, B. J.: Fluxes of methane and carbon dioxide from a small productive lake to the atmosphere, Biogeochemistry, 49, 1–19, 2000.
Fenchel, T., King, G. M., and Blackburn, T. H.: Bacterial biogeochemistry: The Ecophysiology of mineral cycling, Academic Press., 1998.
Gow, A. J. and Langston, D.: Growth history of lake ice in relation to its stratigraphic, crystalline and mechanical structure, USA CRREL Report (Cold Regions Research and Engineering Laboratory), 77(1), 24p, 1977.
Hinkel, K. M.: Ice-cover growth rates at nearshore locations in the Great Lakes, NOAA Tech. Memorandum ERL GLERL, 35, 1983.
IPCC: Intergovernmental Panel on Climate Change (IPCC), the physical science basis, Cambridge Univ. Press., 2007.
Johansson, M., Christensen, T. R., Åkerman, H. J., and Callaghan, T. V.: What determines the current presence or absence of permafrost in the Torneträsk region, a sub-arctic landscape in northern Sweden?, Ambio, 35, 190–197, 2006a.
Johansson, T., Malmaer, N., Crill, P. M., Friborg, T., Akerman, J. H., Mastepanov, M., and Christensen, T. R.: Decadal vegetations changes in a northern peatland, greenhouse gas fluxes and net radiative forcing, Glob. Change Biol., 12, 2352–2369, 2006b.
Juutinen, S., Rantakari, M., Kortelainen, P., Huttunen, J. T., Larmola, T., Alm, J., Silvola, J., and Martikainen, P. J.: Methane dynamics in different boreal lake types, Biogeosciences, 6, 209–223, doi:10.5194/bg-6-209-2009, 2009.
Kling, G., Kipphut, G. and Miller, M.: The flux of CO_2 and CH_4 from lakes and rivers in arctic Alaska, Hydrobiologia, 240, 23–36, 1992.
Kokfelt, U., Rosén, P., Schoning, K., Christensen, T. R., Förster, J., Karlsson, J., Reuss, N., Rundgren, M., Callaghan, T. V., Jonasson, C., and Hammarlund, D.: Ecosystem responses to increased precipitation and permafrost decay in subarctic Sweden inferred from peat and lake sediments, Glob. Change Biol., 15, 1652–1663, doi:10.1111/j.1365-2486.2009.01880.x,

2009.
Langway, C. C. J.: Ice fabrics and the Universal stage, 1958.
Lorrain, R. D., Fitzsimons, S. J., Vandergoes, M. J., and Stievenard, M.: Ice composition evidence for the formation of basal ice from lake water beneath a cold-based Antarctic glacier, Ann. Glaciol., 28, 277–281, 1999.
Lorrain, R., Sleewaegen, S., Fitzsimons, S. and Stievenard, M.: Ice formation in an Antarctic glacier-dammed lake and implications for glacier lake interactions, Arct. Antarct. Alp. Res., 34, 150–158, 2002.
Martinerie, P., Lipenkov, V. Y., Raynaud, D., Chappellaz, J., Barkov, N. I. and Lorius, C.: Air content paleo record in the Vostok ice core (Antarctica): A mixed record of climatic and glaciological parameters, J. Geophys. Res., 99, 10565–10576, 1994.
Mattson, M. D. and Likens, G. E.: Air pressure and methane fluxes, Nature, 347, 718–719, 1990.
Michmerhuizen, C. M., Striegl, R. G., and McDonald, M. E.: Potential Methane Emission from North-Temperate Lakes Following Ice Melt, Limnol. Oceanogr., 41, 985–991, 1996.
Phelps, A. R., Peterson, K. M., and Jeffries, M. O.: Methane efflux from high-latitude lakes during spring ice melt, J. Geophys. Res., 103, 29029–29036, 1998.
Raynaud, D., Delmas, D., Ascencio, J. M., and Legrand, M.: Gas extraction from polar ice cores: a critical issue for studying the evolution of atmospheric CO2 and ice-sheet surface elevation, Ann. Glaciol., 3, 265–268, 1982.
Repo, M. E., Huttunen, J. T., Naumov, A. V., Chichulin, A. V., Lapshina, E. D., Bleuten, W., and Martikainen, P. J.: Release of CO2 and CH4 from small wetland lakes in western Siberia, Tellus B, 59, 788–796, doi:10.1111/j.1600-0889.2007.00301.x, 2007.
Rudd, J. M., Harris, R., and Kelly, C. A.: Are hydroelectric reservoirs significant sources of greenhouse gases?, Ambio, 22, 246–248, 1993.
Sander, R.: Compilation of Henry's Law Constants for Inorganic and Organic Species of Potential Importance in Environmental Chemistry, 1999.
Semiletov, I. P.: Aquatic Sources and Sinks of CO2 and CH4 in the Polar Regions, J. Atmos. Sci., 56, 286–306, 1999.
Sonesson, M., Jonsson, S., Rosswall, T., and Rydén, B. E.: The Swedish IBP/PT Tundra Biome Project Objectives-Planning-Site, Ecol. Bull., 30, 7–25, 1980.
Stumm, W. and Morgan, J. J.: Aquatic Chemistry: Chemical Equilibria and Rates in Natural Waters, 3 Edn., Wiley-Interscience., 1996.

BGD
8, 9639–9669, 2011

Svensson, B. H., Christensen, T. R., Johansson, E., and Ã–quist, M.: Interdecadal Changes in CO_2 and CH_4 Fluxes of a Subarctic Mire: Stordalen Revisited after 20 Years, Oikos, 85, 22–30, 1999.

Walter, K. M., Chanton, J. P., Chapin, F. S., Schuur, E. A. G., and Zimov, S. A.: Methane production and bubble emissions from arctic lakes: Isotopic implications for source pathways and ages, J. Geophys. Res., 113, 16, G00A08, doi:10.1029/2007JG000569, 2008.

Walter, K. M., Smith, L. C., and Stuart Chapin, F.: Methane bubbling from northern lakes: present and future contributions to the global methane budget, Philos. T. R. Soc. A., 365, 1657–1676, 2007.

Walter, K. M., Vas, D. A., Brosius, L., Chapin III, F. S., Zimov, S. A., and Zhuang, Q.: Estimating methane emissions from northern lakes using ice-bubble surveys, Limnol. Oceanogr.-Meth., 8, 592–609, 2010.

Walter, K. M., Zimov, S. A., Chanton, J. P., Verbyla, D., and Chapin, F. S.: Methane bubbling from Siberian thaw lakes as a positive feedback to climate warming, Nature, 443, 71–75, doi:10.1038/nature05040, 2006.

Zimov, S. A., Voropaev, Y. V., Davidov, S. P., Zimova, G. M., Davidova, A. I., Chapin III, F. S., and Chapin, M. C.: Flux of methane from North Siberian aquatic systems: Influence on atmospheric methane, in: Permafrost response on economic development, environmental security and natural resources, edited by: Paepe, R. and Melnikov, V., 511–524, 2001.

BGD
8, 9639–9669, 2011

Gas properties of winter lake ice in Northern Sweden

T. Boereboom et al.

Title Page
Abstract | Introduction
Conclusions | References
Tables | Figures
◀◀ | ▶▶
◀ | ▶
Back | Close
Full Screen / Esc
Printer-friendly Version
Interactive Discussion

Table 1. Bounds for methane fluxes released by the winter lake ice cover. The median value is used if the mean value is higher than the standard deviation.

Methane fluxes ($mg\,CH_4\,m^{-2}\,d^{-1}$)	Minimum	Mean or median	Maximum
Lake 1	$1.34\ 10^{-3}$	3.01	12.7
Lake 2	$3.91\ 10^{-4}$	$4.32\ 10^{-2}$	4.4
Lake 3	$6.52\ 10^{-5}$	$4.35\ 10^{-4}$	$1.14\ 10^{-2}$
Lake 4	$3.59\ 10^{-4}$	$3.21\ 10^{-2}$	4.22

BGD
8, 9639–9669, 2011

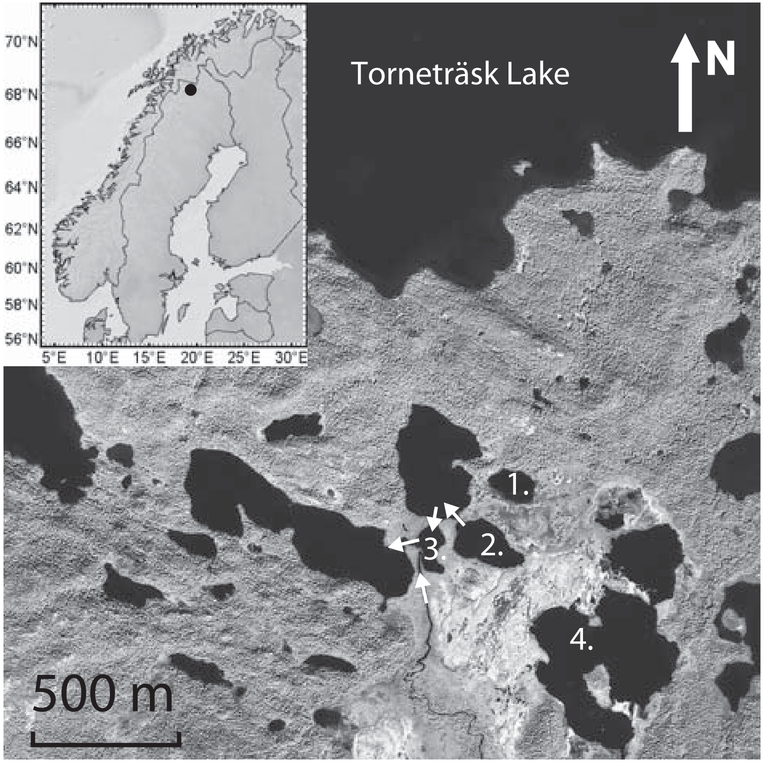

Fig. 1. Location map and lakes configuration (the arrows show water connections). The lakes are all embedded in a mire. Lake 1, small and closed; Lake 2, small and connected to another lake; Lake 3, small, receiving water from a river to the South, connected to another lake to the North and draining into another lake to the West; Lake 4, bigger and closed.

BGD
8, 9639–9669, 2011

Gas properties of winter lake ice in Northern Sweden

T. Boereboom et al.

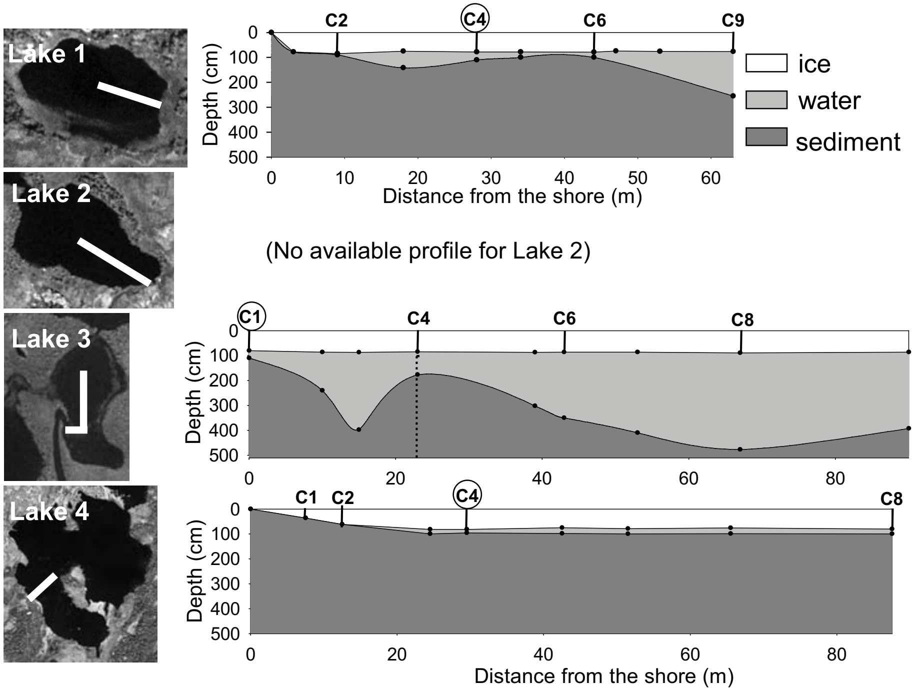

Fig. 2. Lakes geometry along the profiles and ice core sampling locations. The white line on lakes shows the transect direction, letters and numbers correspond to the cores studied for the bubbles morphology and circles indicate cores analyzed for their gas properties. The dotted line in the Lake 3 profile shows the change of azimuth of the transect.

BGD
8, 9639–9669, 2011

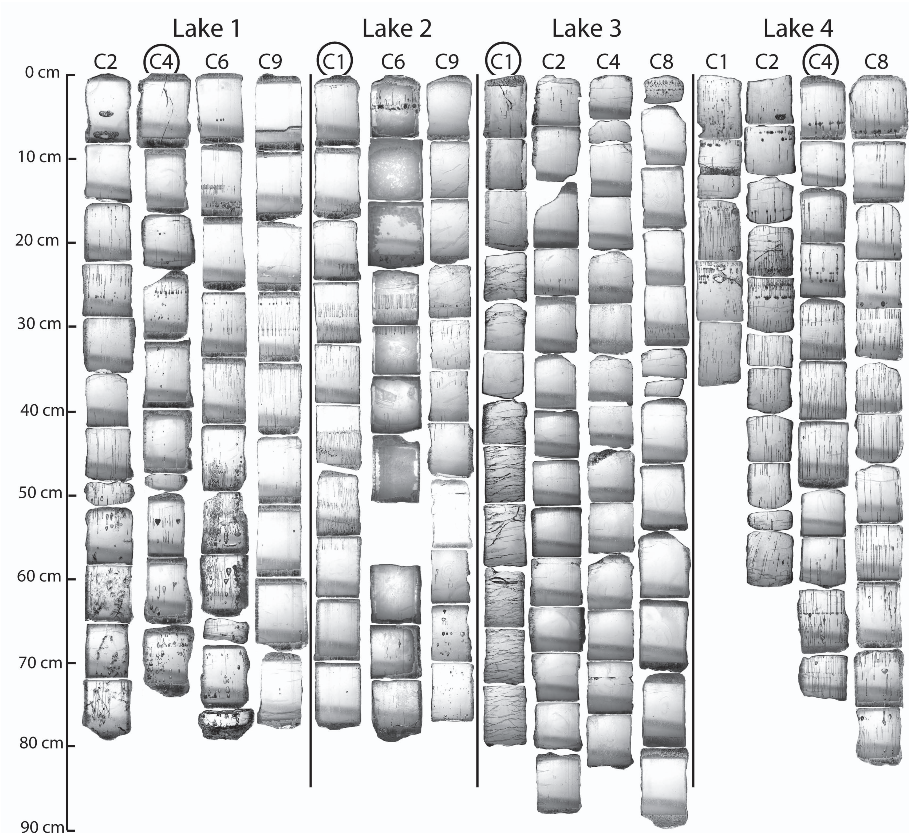

Fig. 3. Ice characteristics, bubbles shapes and dispersion in the 15 studied ice cores (see Fig. 2 for location). Circles denote the cores analyzed at high resolution for their gas properties.

BGD

8, 9639–9669, 2011

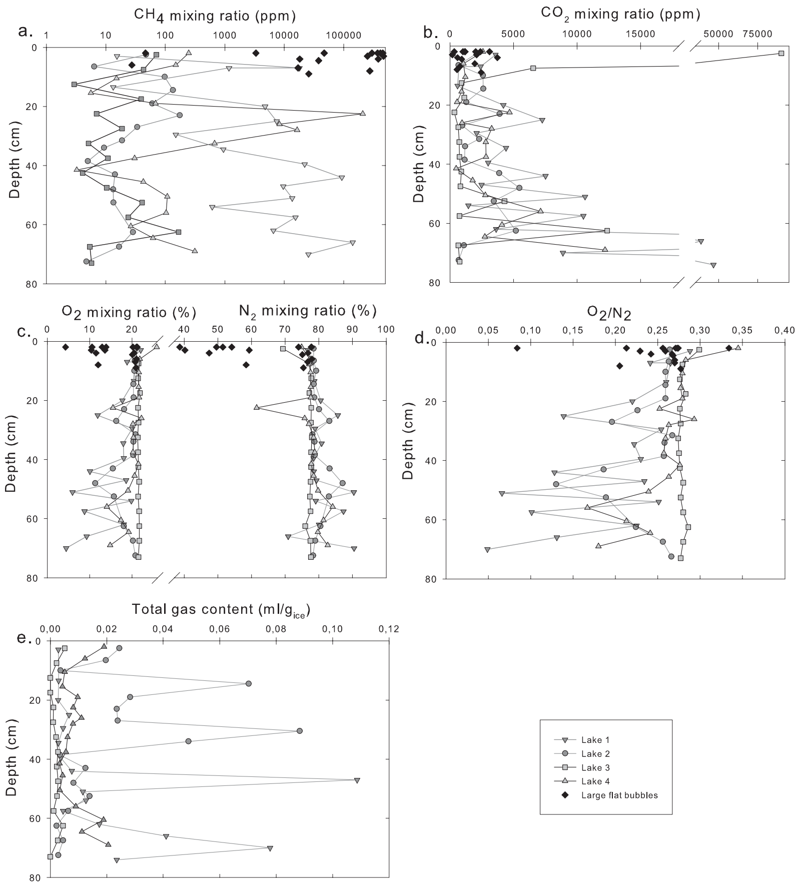

Fig. 4. Gas composition and total gas content versus depth for one core of each of the four studied lakes and for fifteen isolated bubbles sampled near the ice surface. A logarithmic scale has been chosen for CH_4. Note that the total gas content is not presented for the isolated bubbles (see text for details).

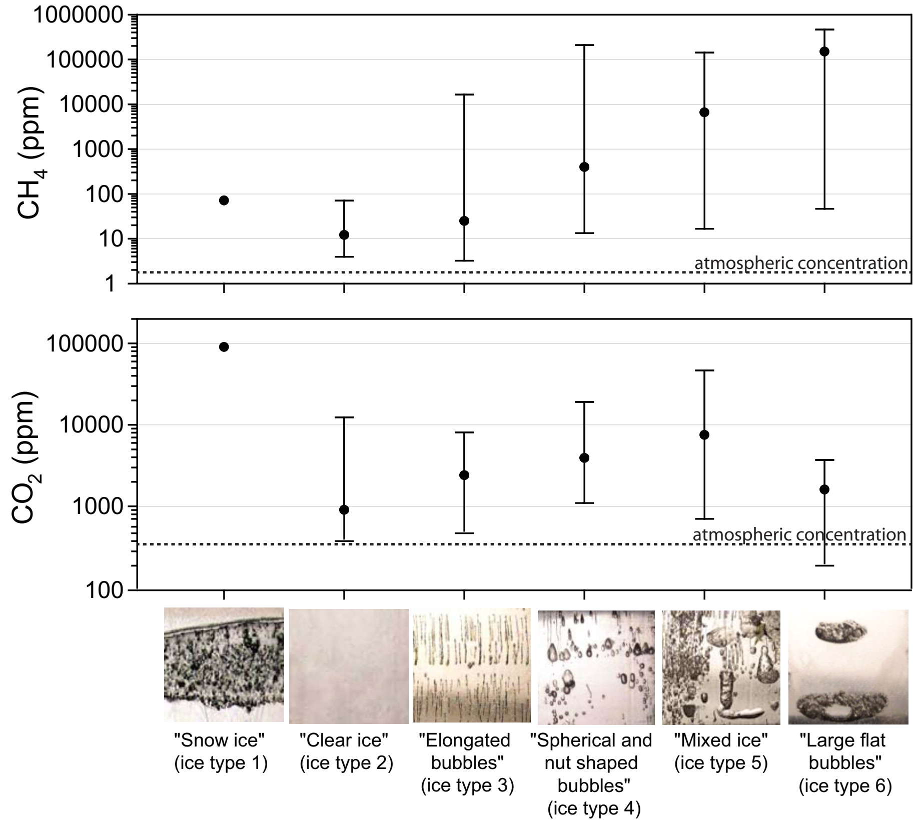

Fig. 5. Ice types classification from bubble shapes and density, with associated ranges of CO_2 and CH_4 mixing ratios. Note the logarithmic mixing ratio scale. Black dots are median values and vertical bars represents the variability in the observations.

BGD
8, 9639–9669, 2011

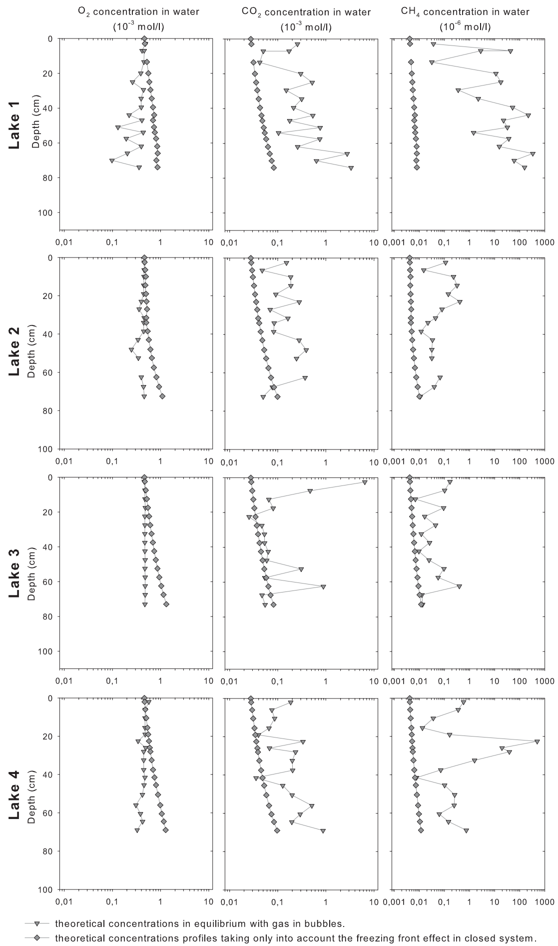

Fig. 6. Theoretical O_2, CO_2 and CH_4 concentrations in water as a function of depth for each lake: gray triangles "down" represent values in equilibrium with measured gas mixing ratios in bubbles (calculated using Henry's law); gray diamonds show values calculated by only taking into account the "reservoir effect" in a closed system (see text for details).

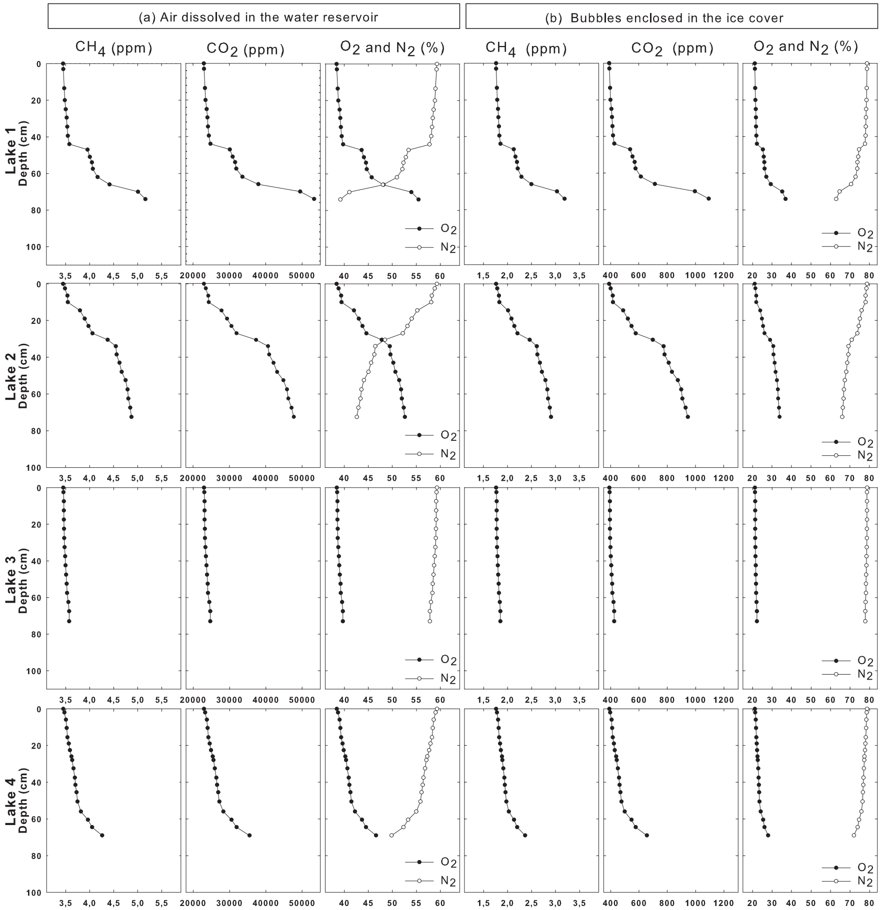

Fig. 7. Theoretical evolution of mixing ratios for **(a)** air dissolved in water and **(b)** bubbles in ice, assuming lakes are closed reservoir, using observed total gas contents for mass balance in ice and assuming no gas fractionation occurs at the ice water interface (see text for details).

BGD

8, 9639–9669, 2011

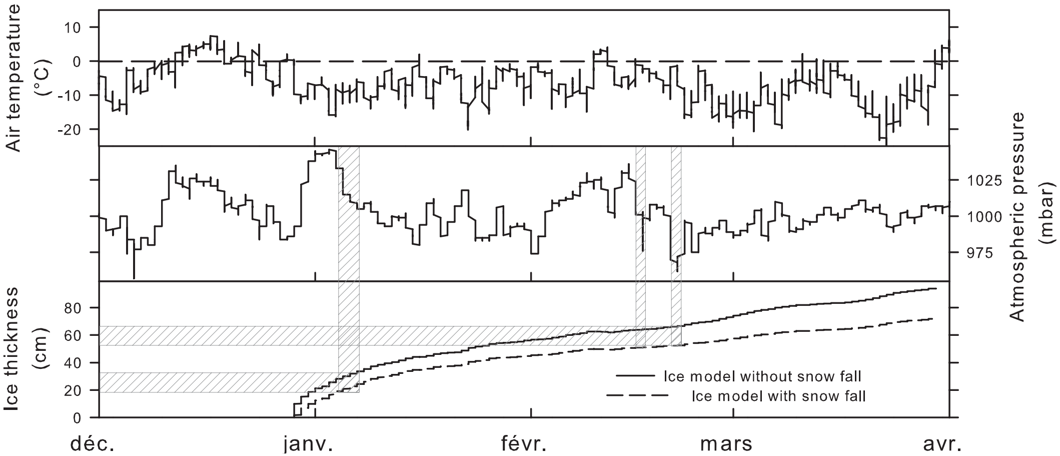

Fig. 8. Air temperature and atmospheric pressure versus modeled ice thickness from Eq. (2) (see text). The dotted line takes snow falls into account. Shadow hatchings show depth fitting with the air pressure drop events. The two highlighted drops correspond with the depth of the two synchronous bubbling events described in the text.